The Astrophysical Journal, 860:73 (9pp), 2018 June 10 https://doi.org/10.3847/1538-4357/aac270

Associating Fast Radio Bursts with Extragalactic Radio Sources: General Methodology and a Search for a Counterpart to FRB 170107

T. Eftekhari, E. Berger, P. K. G. Williams, and P. K. Blanchard
Harvard-Smithsonian Center for Astrophysics, 60 Garden Street, Cambridge, Massachusetts 02138, USA
Received 2018 February 26; revised 2018 May 1; accepted 2018 May 1; published 2018 June 13

Abstract

The discovery of a repeating fast radio burst (FRB) has led to the first precise localization, an association with a dwarf galaxy, and the identification of a coincident persistent radio source. However, further localizations are required to determine the nature of FRBs, the sources powering them, and the possibility of multiple populations. Here we investigate the use of associated persistent radio sources to establish FRB counterparts, taking into account the localization area and the source flux density. Due to the lower areal number density of radio sources compared to faint optical sources, robust associations can be achieved for less precise localizations as compared to direct optical host galaxy associations. For generally larger localizations that preclude robust associations, the number of candidate hosts can be reduced based on the ratio of radio-to-optical brightness. We find that confident associations with sources having a flux density of ∼0.01–1 mJy, comparable to the luminosity of the persistent source associated with FRB 121102 over the redshift range $z \approx 0.1$–1, require FRB localizations of $\lesssim 20''$. We demonstrate that even in the absence of a robust association, constraints can be placed on the luminosity of an associated radio source as a function of localization and dispersion measure (DM). For DM ≈1000 pc cm^{-3}, an upper limit comparable to the luminosity of the FRB 121102 persistent source can be placed if the localization is $\lesssim 10''$. We apply our analysis to the case of the ASKAP FRB 170107, using optical and radio observations of the localization region. We identify two candidate hosts based on a radio-to-optical brightness ratio of $\gtrsim$100. We find that if one of these is indeed associated with FRB 170107, the resulting radio luminosity ($10^{29} - 4 \times 10^{30}$ erg s^{-1} Hz^{-1}, as constrained from the DM value) is comparable to the luminosity of the FRB 121102 persistent source.

Key words: methods: statistical – radio continuum: galaxies

1. Introduction

Fast radio bursts (FRBs) are extremely bright, millisecond-duration pulses of coherent radio emission, with large dispersion measures (DMs) that exceed typical Galactic values, hence pointing to an extragalactic origin. Since the discovery of the first FRB in archival data (Lorimer et al. 2007), roughly 30 additional FRBs have been detected, both in archival and real-time searches (Keane et al. 2012; Thornton et al. 2013; Spitler et al. 2014; Champion et al. 2016; Petroff et al. 2016; Caleb et al. 2017). Despite a growing number of FRB detections, the lack of precise localizations (typically ∼10^3 arcmin^2) has led to a wide range of suggested progenitor systems: giant pulses and magnetar flares (Popov & Postnov 2013; Lyubarsky 2014; Cordes & Wasserman 2016; Lyutikov et al. 2016), mergers of compact objects (Wang et al. 2016; Zhang 2016), the collapse of supramassive neutron stars to black holes (Falcke & Rezzolla 2014), and emission from rapidly spinning magnetars (Kumar et al. 2017; Metzger et al. 2017).

The discovery of the repeating FRB 121102 (Spitler et al. 2014, 2016) led to the first precise localization (Chatterjee et al. 2017) and the identification of a low-metallicity dwarf star-forming host galaxy at $z = 0.193$ (Tendulkar et al. 2017), with properties remarkably similar to the host galaxies of both long-duration gamma-ray bursts (LGRBs) and hydrogen-poor superluminous supernovae (SLSNe) (Metzger et al. 2017). Radio observations with the European VLBI Network (EVN) (VLBI: very longbaseline interferometry) revealed the presence of a compact, persistent radio source with a projected linear size of $\lesssim$0.7 pc, co-located with the bursts to $\lesssim$12 mas (Marcote et al. 2017). The large angular offset between the radio source and the optical center of the galaxy (170–300 mas; Tendulkar et al. 2017) generally argue against an active galactic nucleus (AGN) origin, although this premise is less clear in the case of dwarf galaxies. Similarly, the resulting ratio of radio-to-optical brightness for the persistent source and host galaxy ($L_{\rm rad}/L_{\rm opt} \approx 104$) is much larger than expected for a star formation origin. This has led to the suggestion that the radio source may be a nebula associated with FRB 121102 (Metzger et al. 2017). More recently, the discovery of a large rotation measure with ∼10% variations on half-year timescales suggests the presence of a dynamic and highly magnetized environment surrounding the source of the FRB (Michilli et al. 2018).

The properties of the host galaxy, the repeating nature of the bursts, and the persistent radio source are consistent with a model in which FRBs are powered by young, millisecond magnetars (Metzger et al. 2017; see also Piro 2016; Murase et al. 2016), the same engines that have been argued to power SLSNe and perhaps LGRBs (Nicholl et al. 2017a, 2017b). In this model, individual bursts are emitted via the dissipation of rotational or magnetic energy, while the quiescent radio emission is due to the magnetar wind nebula or the shock interaction between the supernova ejecta and the surrounding circumstellar medium (Beloborodov 2017; Metzger et al. 2017).

In this broad scenario, we expect that FRBs should be located preferentially in dwarf galaxies (Nicholl et al. 2017c) and be coincident with quiescent radio sources similar to that observed in FRB 121102 (Metzger et al. 2017). Nicholl et al. (2017c) demonstrate that $\lesssim$10 FRB localizations will be sufficient to test various formation channels. Given the high event rate for FRBs (∼600 sky^{-1} day^{-1} above 1 Jy; Lawrence et al. 2017) and the improved sensitivities of upcoming telescopes and surveys, the number of detected bursts is expected to increase drastically over

the next few years as new radio facilities come online. However, due to a wide range of localization capabilities, precise localizations will continue to be a challenge.

In Eftekhari & Berger (2017; hereafter, Paper I), we explored how robustly FRBs with different localization regions can be associated with host galaxies based on the optical brightness of the galaxy. Due to the large areal number density of faint optical sources, we showed that sub-arcsecond localizations are required for confident associations with dwarf galaxies at $z \gtrsim 0.1$, whereas localizations of up to $3''$ may suffice if the hosts are instead generally L^* galaxies, where L^* denotes the characteristic luminosity of a bright galaxy.

Here we explore the likelihood of constraining similar associations with radio sources, motivated by the persistent radio source associated with FRB 121102 and assuming that all FRBs are coincident with such sources, potentially with a resulting high radio-to-optical flux ratio. We also explore what limits can be placed on the presence and luminosity of a persistent radio source (as a function of localization area) even in the absence of a robust association. We assess our results in the context of existing and upcoming radio facilities. As an example of our method, we present radio (Very Large Array (VLA)) and optical (*Magellan*) observations of the localization region of the ASKAP FRB 170107 (Bannister et al. 2017). We search for radio counterparts in the region using the radio-to-optical flux ratio to identify potential candidates.

The paper is structured as follows. We begin by using radio source number counts to determine the probability of chance coincidence for an FRB and a persistent radio source as a function of localization region and persistent source flux density (Section 2). In Section 3 we use these results to constrain the upper limit on the radio luminosity of a source in the absence of a robust association. In Section 4, we discuss various techniques which may further aid in the identification of associated counterparts. We present an example of our approach in Section 5, using radio and optical observations of the localization region of FRB 170107. Finally, we discuss our results in the context of existing and planned FRB search facilities in Section 6.

2. Assessing the Probability of Chance Coincidence with Radio Source Counts

We assess the likelihood that an FRB is associated with a persistent radio source by calculating the probability of chance coincidence for a source of a given brightness within a localization region. We use the 1.4 GHz Euclidean-normalized differential source counts presented in Condon et al. (2012) to calculate the number density of radio sources above some limiting flux density, $n(\geqslant S)$; see the top left panel of Figure 1. These source counts are measured over the range 10 μJy–100 Jy and extrapolated to lower flux densities, imposing an evolutionary model for the spectral luminosity function of extragalactic radio sources (Condon 1984a, 1984b). The source counts are comprised of both AGN and star-forming galaxies, with the latter dominating the counts below $\sim$0.1 mJy (Padovani et al. 2015), although radio-quiet AGN have been shown to comprise a sizable fraction of the sub-mJy population (Fomalont et al. 2006; Padovani et al. 2007, 2015; Smolčić et al. 2008). We assume a Poisson distribution of radio sources across the sky and calculate the chance coincidence probability as:

$$P_{\rm cc} = 1 - e^{-\pi R^2 n(\geqslant S)}. \quad (1)$$

The localization region, R, is parameterized by $R = 2R_{\rm FRB}$, where $R_{\rm FRB}$ is the 1σ localization radius of the FRB.[1]

Using the integrated source counts, we plot in the top right panel of Figure 1 the number of radio sources above some limiting flux density [i.e., $\pi R_{\rm FRB}^2 n(\geqslant S)$] as a function of $R_{\rm FRB}$. We plot the results over the range $S = 1$ μJy to 1 Jy, in order of magnitude increments. We find an expectation value of about one source at $S \approx 100$ mJy within the typical localization regions of single-dish telescopes ($R_{\rm FRB} \approx 10'$). Conversely, at the faint end ($\approx$0.1 mJy), we expect one source within $R_{\rm FRB} \approx 1'$.

We plot the resulting chance coincidence probability contours as a function of flux density and R in the lower panel of Figure 1. We denote the contours corresponding to $P_{\rm cc} = 0.01$ and 0.1. We also show the flux density of the persistent radio source associated with FRB 121102 over the redshift range $z \approx 0.1$–1, as well as the nominal sensitivities for a number of existing and future radio observatories. We note that the FRB 121102 persistent source falls well below $P_{\rm cc} = 0.01$. While most existing facilities are sensitive to FRB 121102-like persistent sources across a range of redshifts ($z \approx 0.1$–1; see Table 1), detecting such a source at $z \sim 1$ (with an expected flux density of a few μJy) is challenging even with the VLA. On the other hand, the advent of the ngVLA and SKA will push the achievable sensitivity to sub-μJy levels, and hence the detection of such persistent sources to $z \gtrsim 1$.

At $\lesssim$1 mJy (i.e., FRB 121102-like persistent sources at $z \gtrsim 0.1$), confident associations ($P_{\rm cc} \lesssim 0.01$) require localizations of $R \lesssim 20''$. At higher redshifts ($z \sim 1$), localizations of $R \lesssim 1''$ are required. While this level of localization is not feasible for most FRB search telescopes, it can be achieved using the VLA in an extended configuration, or with VLBI, as in the case of FRB 121102, which was localized to $\lesssim$12 mas (Marcote et al. 2017). However, a number of facilities, including the VLA, MeerKAT, ASKAP, and DSA-10, will be able to provide the $\lesssim 20''$ localizations required for robust associations with sub-mJy sources at moderate redshifts ($z \sim 0.5$). Conversely, at $R \gtrsim 1'$, confident associations with sub-mJy sources are not feasible. This corresponds to the localization regime for CHIME, UTMOST-2D, and Apertif (as well as single-dish telescopes). These facilities can provide robust associations only if the counterparts generally have flux densities of $\gtrsim$1 mJy, but this would require some of the persistent radio counterparts to be much more luminous than the source associated with FRB 121102. Finally, the poor localizations from single-dish telescopes are insufficient for robust associations with all but the brightest ($\sim$Jy) sources. Although these telescopes may reveal additional bursts from FRBs in the case of repetitions, they will not be able to directly provide localizations that will lead to associations with persistent radio sources at any reasonable confidence level.

In Table 1, we list a number of radio facilities designed to detect FRBs. We sort these by anticipated or known

[1] Note that we assume uniform sensitivity across an area with radius $R_{\rm FRB}$. In practice, this implies that the localization region has been uniformly imaged via mosaicking, for instance. In the Appendix, we repeat the analysis presented here, taking into account the primary beam response of the telescope. We find that the assumption of uniform sensitivity is justified, with a more accurate beam model resulting in negligible differences.

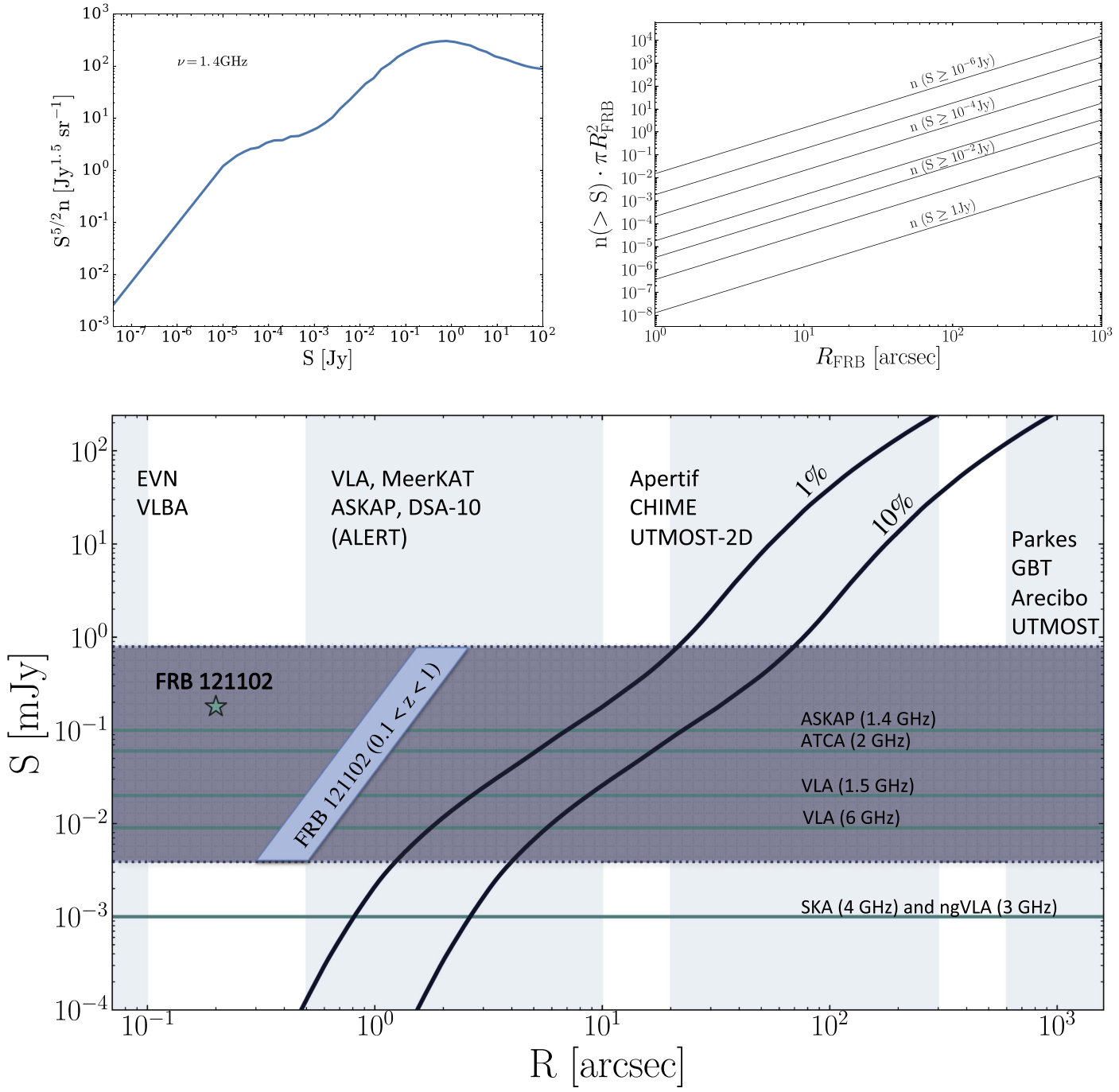

Figure 1. Top left: Euclidean-normalized differential radio source counts (including contributions from AGN and star-forming galaxies) at 1.4 GHz (Condon et al. 2012). Top right: the number of radio sources brighter than a limiting flux density S [$n(>S)\pi R_{\rm FRB}^2$)] as a function of FRB localization radius ($R_{\rm FRB}$). Individual lines correspond to order of magnitude increments, spanning from 1 μJy to 1 Jy. Bottom: probability contours for $P_{\rm cc} = 0.01$ and 0.1 as a function of flux density (S) and radius (R). We also plot the VLA localization and flux density for the quiescent radio source associated with FRB 121102. Vertical bars indicate the localization regimes of various radio telescopes that are designed to detect or capable of detecting FRBs (Table 1). Localizations below 20″ are required for robust associations with radio sources below 1 mJy. Also shown as horizontal lines are the 3σ sensitivities for a number of follow-up facilities (assuming 1 hr observations for each).

localization capability. We also list the flux density of a radio source in the respective localization region that would have $P_{\rm cc} = 0.01$ and 0.1, as well as the maximum redshift $z_{\rm max}$ out to which an association with an FRB 121102-like persistent source can be made. These values are extracted directly from the probability contours in Figure 1. We find that while the VLA, ASKAP, DSA-10, and MeerKAT are capable of probing these sources out to $z \sim 1$ (and $z > 1$ for VLBI), the large flux densities required for $P_{\rm cc} \approx 0.01$ for facilities with localizations of $R \gtrsim 1'$ preclude associations with these sources at $z \gtrsim 0.1$. Given the expectation from radio source number counts and the sensitivity of current instruments, localizations below 3″ will not improve the association confidence markedly, as existing facilities cannot achieve the μJy levels required for $P_{\rm cc} \lesssim 0.1$.

We note that for the same localization requirement of $R \lesssim 20''$, optically based host galaxy associations are impractical, requiring host luminosities several times brighter than L^*

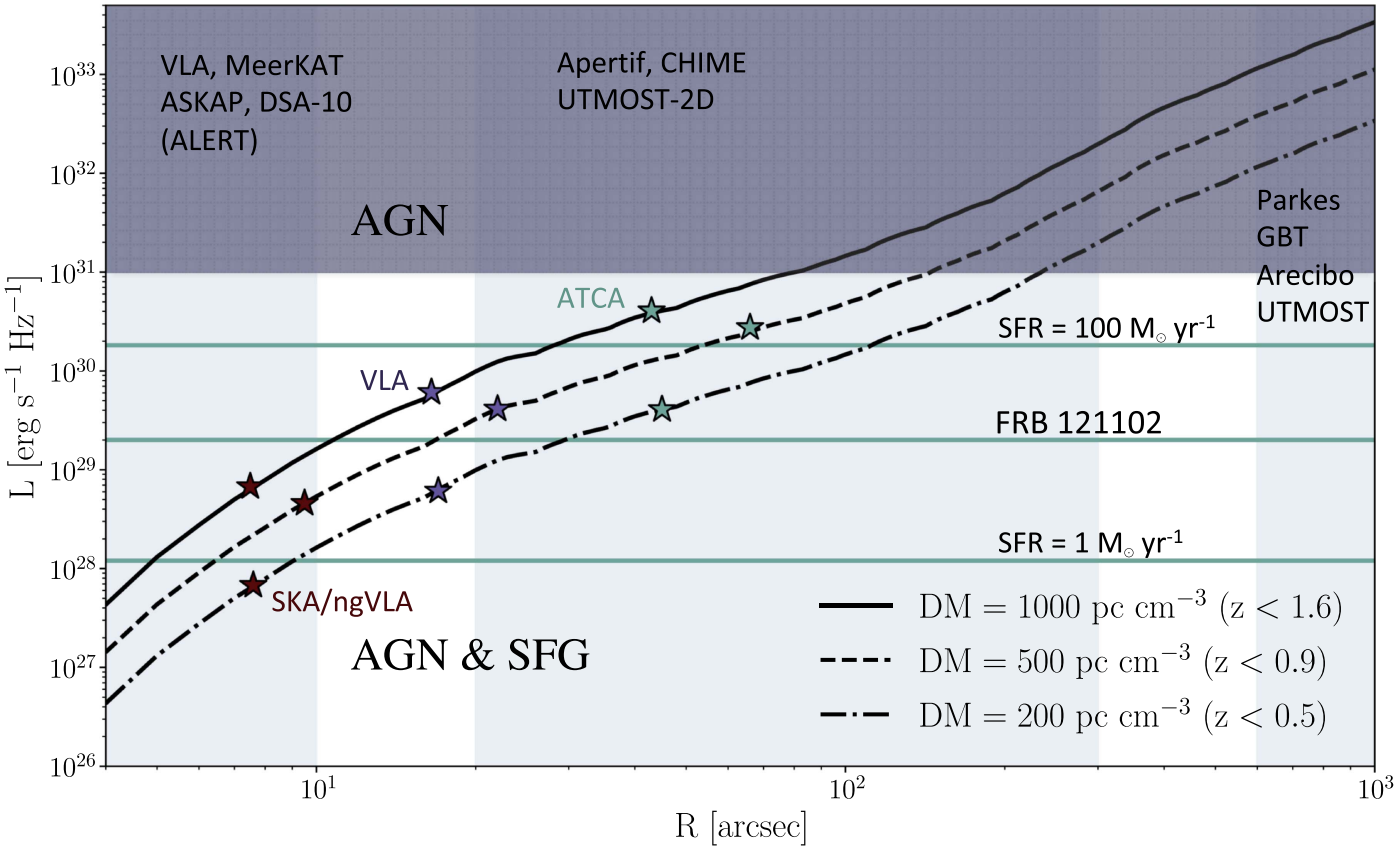

Figure 2. Upper limit on the luminosity of an associated radio source as a function of localization radius for a range of DM values. The limit is calculated using the number counts in Figure 1 set to an expectation value of one source and the upper limit on the redshift for each DM value. We plot as horizontal lines the luminosity of the quiescent radio source associated with FRB 121102 and the luminosities for star-forming galaxies with star formation rates of 1 and 100 $M_\odot$ yr^{-1}. We also indicate the dividing line above which radio sources are almost all AGN ($L \approx 10^{31}$ erg s^{-1} Hz^{-1}). Vertical bars indicate the localization regimes of various radio telescopes that are designed to or capable of detecting FRBs (Table 1). Also shown are the achievable luminosity limits (for each DM, or equivalently $z_{\rm max}$) for follow-up observations with ATCA, VLA, and the SKA/ngVLA.

Table 1
Radio Facilities and Their Localization Capabilities

Telescope	$R_{\rm FRB}$ (arcsec)	$S(P_{\rm cc} = 0.01)$ (mJy)	$S(P_{\rm cc} = 0.1)$ (mJy)	$z_{\rm max}$ ($P_{\rm cc} = 0.01$)
VLBA/EVN	0.001–0.1	$<10^{-4}$[a]	$<10^{-4}$[a]	>1
VLA	0.1–3	0.01	$<10^{-4}$[a]	0.6
ASKAP	0.8–1.5	0.03	0.002	0.4
DSA-10	1–2	0.04	0.005	0.4
MeerKAT	2–10	0.2	0.03	0.2
UTMOST-2D	2–30	2	0.2	0.1
Apertif[b]	5–60	20	0.8	$z < 0.1$
CHIME	20–600	200	30	$z < 0.1$
UTMOST	100–300	400	60	$z < 0.1$
Arecibo	200–230	500	100	$z < 0.1$
Parkes	500–800	1000	400	$z < 0.1$
GBT	500–800	1000	400	$z < 0.1$

Notes. Radio facilities capable of detecting FRBs, ordered by approximate localization capability.
[a] Limits are used to denote flux values which extend below the radio source number counts.
[b] In conjunction with LOFAR, the Apertif LOFAR Exploration of the Radio Transient Sky (ALERT) survey can provide more accurate (arcsecond) localizations (van Leeuwen 2014; see also http://alert.eu/).

at redshifts below $z \lesssim 0.1$ (Paper I). Assuming that FRB 121102 is representative of the FRB population as a whole, and that we can expect continuum radio sources coincident with FRBs, the lower areal number density of radio sources on the sky enables more robust associations at a given localization precision; we demonstrate this further using optical and radio observations of the localization region of FRB 170107 in Section 5.

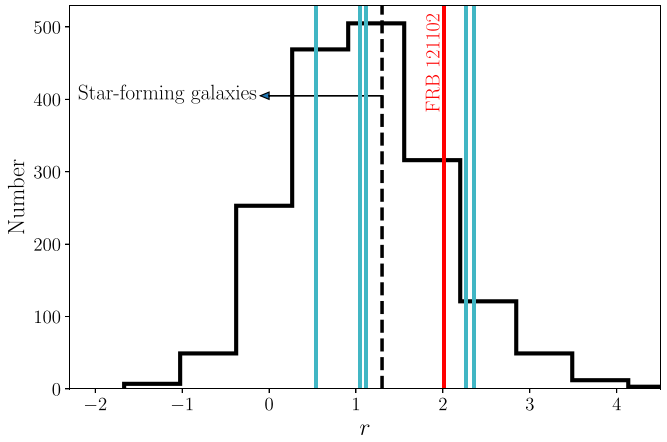

Figure 3. Distribution of the radio-to-optical flux ratio [$r = \log(S_{1.4\ \mathrm{GHz}}/S_V)$] for 1784 radio sources from the literature (Machalski & Condon 1999; Afonso et al. 2005; Padovani et al. 2009). The dashed line indicates the nominal maximum value for star-forming galaxies. Blue lines correspond to the five radio sources that we identified in the localization region of FRB 170107 (see Table 2). Also shown in red is the ratio for the persistent source associated with FRB 121102.

3. Placing an Upper Limit on the Radio Luminosity

We use the results of Section 2 to investigate upper limits on the radio luminosity of an associated persistent source in the absence of a robust association. For a given localization radius, we determine the typical brightest source expected within the region (using the top right panel of Figure 1). For a given intergalactic DM value (excluding the host and Milky Way contribution), we then estimate z_{max}, using the DM–redshift relation of Deng & Zhang (2014; see also Ioka 2003) and incorporating the uncertainty due to intergalactic medium inhomogeneities as parameterized by McQuinn (2014). We follow the procedure described in detail in Paper I. In Figure 2, we plot the maximum luminosity of a radio source as a function of R for a range of DM values. As in Figure 1, we overlay the localization capabilities of the various FRB search facilities for reference. We also denote lines corresponding to the luminosity of star-forming galaxies with star formation rates of 1 and 100 $M_\odot\ \mathrm{yr}^{-1}$, and we indicate the dividing line above which radio sources are almost exclusively AGN ($L \approx 10^{31}\ \mathrm{erg\ s^{-1}\ Hz^{-1}}$). Finally, we mark the achievable luminosity limits as a function of redshift for several facilities (ATCA, VLA, and the SKA/ngVLA).

The results suggest that for DM $\approx$ 1000 pc cm^{-3}, an upper limit comparable to the luminosity of the FRB 121102 persistent radio source ($L \approx 2 \times 10^{29}\ \mathrm{erg\ s^{-1}\ Hz^{-1}}$; Marcote et al. 2017) can be placed if $R \lesssim 10''$. These limits would also rule out star formation at the level of $\approx$100 $M_\odot\ \mathrm{yr}^{-1}$. A similar localization in the optical would only constrain the host galaxy luminosity to $\approx L^*$ (see Paper I and Figure 3). However, these limits are below the nominal sensitivities for existing radio telescopes. For example, although the VLA can provide the required localization precision, the 3σ limiting flux density at 6 GHz corresponds to a luminosity upper limit of $L \approx 6 \times 10^{29}\ \mathrm{erg\ s^{-1}\ Hz^{-1}}$. For lower DMs, similar constraints on the luminosity of a quiescent radio source can be placed for larger localizations, i.e., $R \lesssim 30''$ for DM $\approx$200 pc cm^{-3}.

Although the upcoming SKA and ngVLA will provide the sensitivities required for meaningful upper limits, similar limits can be placed with existing facilities, only for lower DM values (DM $\lesssim$ 500 pc cm^{-3}).

4. Rejecting Spurious Radio Associations

While the probability of chance coincidence analysis in Section 2 provides a direct measure of the confidence level of associating an FRB with a persistent radio source, we are also interested in exploring additional ways of rejecting spurious associations with unrelated radio emission due to AGN or star-forming galaxies (i.e., the sources that make up the extragalactic radio source counts). First, we discuss a number of methods that can be used to identify radio emission due to star formation and separate these sources from FRB host candidates. Next, we discuss the distinction between AGN and putative FRB hosts, which is generally more complicated due to the wide range of AGN radio properties.

4.1. Rejecting Star-forming Galaxies

Motivated by the properties of the FRB 121102 persistent radio counterpart, the ratio of radio-to-optical flux can be used to rule out radio emission due to star formation. This ratio, commonly defined as $r \equiv \log(S_{1.4\ \mathrm{GHz}}/S_V)$, where S_V is the V-band flux density, has previously been used as a discriminant between radio-loud AGN and star-forming galaxies, where the latter have $r < 1.4$ (Machalski & Condon 1999; Afonso et al. 2005; Barger et al. 2007; Seymour et al. 2008; Vega et al. 2008; Padovani et al. 2009). In Figure 3, we plot the distribution of radio-to-optical flux ratios for radio sources from the literature (Machalski & Condon 1999; Afonso et al. 2005; Padovani et al. 2009) and for the FRB 121102 persistent source (Chatterjee et al. 2017). In the case of FRB 121102, the presence of bright radio emission, coupled with a faint optical host, leads to $r \approx 2.0$ and implies that the radio emission does not arise from star formation. Assuming that this is generally the case for FRB counterparts, we can set a threshold of $r \gtrsim 1.4$ which effectively reduces the source counts by a factor of about two.

The angular extent of the radio emission can also be used to distinguish star-forming galaxies from compact FRB radio counterparts (Ofek 2017). The radio emission from the latter will have a scale of $\lesssim$1 pc, as in the case of FRB 121102 ($\lesssim$0.7 pc; Marcote et al. 2017), appearing as unresolved sources. Star-forming regions at this scale would point to extremely high star formation rates per unit area ($\sim 10^{5-7}\ M_\odot\ \mathrm{yr}^{-1}\ \mathrm{kpc}^{-2}$; Park et al. 2016). This level of star formation activity is expected in only the most extreme star-forming regions (Varenius et al. 2014). This argument is borne out by VLBI observations, which show that about 80% of radio sources brighter than 1 mJy are resolved, thereby implicating extended regions of star formation or FRII AGN (Deller & Middelberg 2013). Thus, VLBI follow-up of any candidate FRB counterparts can be used to reject extended radio sources.

4.2. Rejecting AGN

The wide range of radio emission properties in AGN makes their rejection more challenging. For example, the radio-to-optical flux ratios for AGN exhibit a range of values. Keane et al. (2016) claimed the first precise localization of an FRB based on the detection of a contemporaneous radio counterpart within the Parkes Telescope localization region. The counterpart was subsequently shown to be a variable AGN undergoing strong refractive scintillation (Williams & Berger 2016). A search for counterparts in the FRB 131104 localization region similarly revealed a coincident variable AGN (Shannon & Ravi 2017). The approach we advocate here is to use various

multi-wavelength data to argue whether a source is consistent with an AGN, and hence not securely associated with an FRB.

Optical emission lines can be used to identify AGN using the Baldwin, Phillips & Terlevich (BPT) diagram (Baldwin et al. 1981). However, if we impose a high radio-to-optical flux ratio, then obtaining optical spectra of the associated host galaxies at $z \gtrsim 0.5$ will be beyond the reach of most ground-based facilities.

Sources that are precisely coincident with the nuclei of their host galaxies are more likely to have an AGN origin. However, this is less clear in the case of dwarf galaxies in which the radio source may be offset from the optical center of the galaxy (Reines et al. 2011) and the optical center may not be well defined. The fraction of dwarf galaxies that host AGN is thought to be quite small, with an occupation fraction of 0.5%–3% (Reines et al. 2013; Pardo et al. 2016).

Finally, X-ray observations can be used to discern AGN activity, with X-ray luminosities of $L_X \gtrsim 10^{42}\,\mathrm{erg\,s^{-1}}$ indicative of AGN, although low-luminosity AGN may exhibit lower values. In the case of FRB 121102, X-ray emission is not detected, corresponding to a 3σ upper limit of $L_X \lesssim 3 \times 10^{41}\,\mathrm{erg\,s^{-1}}$ at 0.5–10 keV (Chatterjee et al. 2017). The possibility of a low-luminosity, radio-loud AGN cannot be precluded from this result, however. In general, the absence of detectable X-ray emission may not be constraining, while a direct detection can be used to argue for an AGN origin.

5. A Practical Example: FRB 170107

FRB 170107 (Bannister et al. 2017) was the first FRB detected by the Australian Square Kilometer Array Pathfinder (ASKAP; Johnston et al. 2008; Schinckel et al. 2012) using the phased array feed system. This led to the detection of the pulse in three separate beams, allowing for a localization region smaller than the size of an individual beam: the 90% confidence ellipse has semimajor and semiminor axes of $5\farcm3 \times 4\farcm2$ with a position angle of 52°. Motivated by the smaller size of the localization region compared to previous FRBs and the analysis presented above, we obtained radio and optical follow-up observations shortly after publication of the event to search for a host galaxy via a radio source with a large radio-to-optical flux ratio.

5.1. Radio Observations

We obtained radio observations with the Karl G. Jansky VLA[2] on 2017 June 2, 146 days after the FRB. The observation lasted 30 minutes and the pointing center was R.A. = 11:23:10, decl. = −05:01:00, matching the FRB position centroid reported by Bannister et al. (2017). The correlator was configured in the standard "*C* band" wideband continuum mode using the 3-bit samplers, covering the full bandwidth of 4–8 GHz. Standard calibration techniques were used. The bandpass and flux density calibrator was 3C 286 and the complex gain calibrator was the blazar PKS J1131−0500.

After this observation was conducted, we were provided with an updated localization probability map with a new centroid that differed from the published position (R. Shannon and K. Bannister, 2017, private communication). On 2017 June 22 we conducted a second observation using the improved pointing center of R.A. = 11:23:21, decl. = −04:58:38. The two positions were separated by almost exactly the half-width at half power of the VLA at 6 GHz. The other characteristics of this observation were identical to those of the first.

We calibrated and imaged both observations within the CASA software environment (McMullin et al. 2007) using standard techniques. We imaged the fields separately, creating images of 1024×1024 pixels at a scale of $1''$ per pixel using multi-frequency synthesis (Sault & Wieringa 1994) and *w*-projection with 128 planes (Cornwell et al. 2008). The images of the first and second pointing centers achieved rms values of 8 and 10 μJy at the pointing center, respectively.

We visually identified radio sources and measured their flux densities following a primary beam correction. Due to the decrease in sensitivity away from the pointing center, we imposed a 75 μJy threshold and found five radio sources above this limit. The radio image from our second observation (2017 June 22) is shown in Figure 4 and the identified sources are listed in Table 2.

5.2. Optical Observations

We obtained *i*-band observations covering the FRB localization region with IMACS on the 6.5 m *Magellan* Baade Telescope. We processed the images using standard procedures in `IRAF` and calibrated the resulting magnitude measurements using field stars in common with the Pan-STARRS1 3π survey. We identify optical counterparts to three of the five radio sources (see Figure 4). We list the apparent *i*-band magnitudes (corrected for Galactic extinction[3]; Schlafly & Finkbeiner 2011) for each source in Table 2. The two optical non-detections correspond to a 3σ limiting magnitude of 24.3 mag.

5.3. Candidate Sources

Based on the flux densities of the detected sources (76–158 μJy), we estimate the expected number of sources above 75 μJy from the radio source number counts. To compare our sources at 6 GHz to the expectation from the 1.4 GHz source counts, we assume a spectral index of $\alpha = -0.7$ (Condon et al. 2012), corresponding to an effective limiting flux density of 210 μJy at 1.4 GHz. From our analysis in Section 2, we therefore expect to find around seven radio sources in the localization region, consistent with our results. The flux densities of the detected sources preclude a robust association, however. Namely, even for the brightest detected source, $P_{\rm cc} \approx 0.99$; $P_{\rm cc} = 0.01$ requires a ≈0.1 Jy source.

Motivated by the persistent radio source associated with FRB 121102, we determine the ratio of radio-to-optical flux, $r = \log(S_{6\ \rm GHz}/S_i)$, for each source. Of the five identified radio sources, two lack optical counterparts, corresponding to large radio-to-optical flux ratios ($r \gtrsim 2.3$ and $r \gtrsim 2.4$), comparable to the value observed for the FRB 121102 counterpart ($r \approx 2.0$) and well in excess of expected values for star-forming galaxies (see Figure 3). Conversely, the three sources with optical counterparts have $r \lesssim 1.1$, within the regime of star-forming galaxies. We therefore consider the two radio sources with optical non-detections as potential hosts of FRB 170107, given that we can rule out star formation as the

[2] The VLA is operated by the National Radio Astronomy Observatory, a facility of the National Science Foundation operated under cooperative agreement by Associated Universities, Inc. The observations presented here were obtained as part of program VLA/17A-453.

[3] http://irsa.ipac.caltech.edu/applications/DUST/

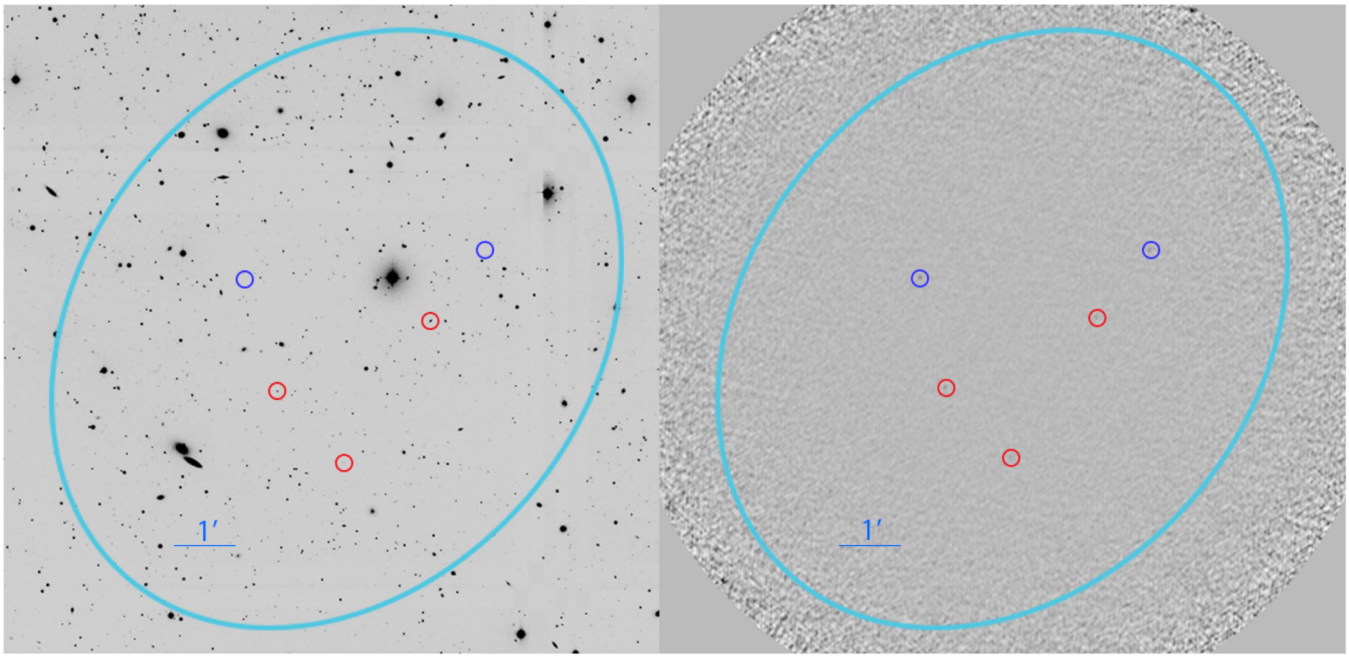

Figure 4. Optical (left) and radio (right) images of the 90% ASKAP localization region for FRB 170107 (cyan) with a pointing center given by R.A. = 11:23:21, decl. = −04:58:38. A total of five sources are identified in the radio image. Blue circles correspond to candidate counterparts based on high radio-to-optical flux ratios; red circles correspond to sources with ratios typical of star-forming galaxies.

Table 2
Radio Sources in the FRB 170107 Localization Region

R.A.	Decl.	Flux Density [μJy]	m_i	r
11:23:14.739	−04:58:20.47	86 ± 15	20.4	0.5
11:23:24.431	−04:59:33.21	112 ± 15	21.4	1.0
11:23:20.400	−05:00:38.59	76 ± 14	22.0	1.1
11:23:11.227	−04:57:14.38	129 ± 23	>24.3	>2.3
11:23:26.385	−04:57:41.65	158 ± 16	>24.3	>2.4

Note. Optical non-detections are listed as the 3σ limiting magnitude.

source of the radio emission. We refer to the 158 and 129 μJy sources as G1 and G2, respectively.

Assuming a nominal host DM contribution of $\sim$100 pc cm^{-3} (as in Bannister et al. 2017), we estimate an upper bound on the redshift using the same approach as in Section 3. We find that the DM-inferred redshift can be characterized as a normal distribution with $\langle z \rangle \approx 0.54$ and a 68% confidence range of 0.18–0.90. The range of possible luminosities is therefore $1 \times 10^{29} - 4 \times 10^{30}$ erg s^{-1} Hz^{-1}, comparable to the luminosity of the FRB 121102 persistent source ($L \approx 2 \times 10^{29}$ erg s^{-1} Hz^{-1}; Marcote et al. 2017). The mean luminosities (assuming $z \approx 0.54$) are 1.3×10^{30} erg s^{-1} Hz^{-1} and 1.0×10^{30} erg s^{-1} Hz^{-1} for G1 and G2, respectively.

The 3σ limiting magnitudes in the optical ($m_i > 24.3$) correspond to $\approx$0.1 L^* at $z \approx 0.54$ (or $\approx$0.01L^* at $z \approx 0.18$ and $\approx$0.3 L^* at $z \approx 0.90$). These are broadly consistent with the host galaxy of FRB 121102 which has a luminosity of $\approx$0.01 L^* (Tendulkar et al. 2017).

As both the radio and optical properties of our candidate sources are consistent with the properties of the FRB 121102 host galaxy and radio counterpart, we argue that these sources are viable counterparts to FRB 170107. The large localization precludes a robust association with either source, however, given that the expectation value for such a source is >1 (Section 2). Targeted follow-up observations with radio interferometers may reveal additional bursts from these sources, leading to an unambiguous host identification.

6. Conclusions

Motivated by the persistent radio source associated with the repeating FRB 121102, we explored the likelihood of identifying persistent radio sources associated with FRBs as a function of their flux density and the FRB localization radius, assuming that all FRBs are associated with such sources. We also quantified the limits that can be placed on a radio counterpart in the absence of a robust association. Finally, we applied our analysis to the case of FRB 170107. Our main results can be summarized as follows.

1. Localizations of $R \lesssim 20''$ are required for robust associations ($P_{\rm cc} = 0.01$) with sub-mJy radio sources at $z \approx 0.1$. At higher redshifts ($z \approx 1$), smaller localizations of $R \approx 1''$ are needed. A number of radio facilities, including the VLBA, EVN, VLA, MeerKAT, ASKAP, and DSA-10 will be capable of providing such FRB localizations. For large localizations ($\approx 300''$), only bright sources ($\approx$10–100 Jy) lead to $P_{\rm cc} \lesssim 0.01$. However, such sources are not obviously expected given the luminosity of the FRB 121102 counterpart and the expected extragalactic redshifts. Nevertheless, several radio facilities, including Apertif, CHIME, and UTMOST-2D will be able to achieve this level of accuracy.
2. Radio sources with luminosities similar to the FRB 121102 persistent source beyond $z \sim 0.5$ are not easily detectable with existing facilities, since they will have flux densities of only a few μJy. However, the upcoming SKA and ngVLA will be sensitive to such sources beyond $z \sim 1$.

3. In the absence of a robust association, an upper limit can be placed on the radio luminosity of an associated radio source. These limits are particularly interesting for localizations of $R \lesssim 10''$ (for DM $\approx$ 1000 pc cm^{-3}) or $R \lesssim 30''$ (for DM $\approx$ 200) where the luminosity is comparable to that of the FRB 121102 persistent source. Conversely, in the optical, a $10''$ localization does not place a particularly meaningful constraint on the host galaxy luminosity (upper limit of L^* for DM $\approx$ 1000 pc cm^{-3}; Paper I). These limits are below the imaging capabilities of existing facilities, however, except for low DM values (DM $\lesssim$ 500 pc cm^{-3}).
4. A number of multi-wavelength techniques can be used to reject spurious associations with unrelated radio sources, namely AGN and star-forming galaxies. The radio-to-optical flux ratio can be used to reject star-forming galaxies as FRB host candidates, imposing a threshold of $r \gtrsim 1.4$ for FRB counterparts. Although the rejection of AGN is generally more challenging, optical emission lines and X-ray observations can be leveraged to determine whether a source is consistent with an AGN.
5. Using a combination of radio and follow-up observations, we identified five radio sources above 75 μJy within the FRB 170107 localization region. Two of these sources share properties consistent with the FRB 121102 persistent source, namely a high radio-to-optical flux ratio, a comparable radio luminosity, and a low-luminosity optical counterpart. We find that the range of allowed radio luminosities (1×10^{29}–4×10^{30} erg s^{-1} Hz^{-1}) is comparable to that of the FRB 121102 persistent source (2×10^{29} erg s^{-1} Hz^{-1}). Similarly, the optical limits ($m_i > 24.3$ mag) are consistent with the dwarf host galaxy of FRB 121102 ($m_r \approx 23.3$ mag).

Combined radio and optical follow-up observations of FRB localization regions can provide a powerful tool for identifying host associations. If FRB 121102 is representative of the FRB population, candidate sources can be identified on the basis of their radio-to-optical flux ratio, and targeted follow-up observations can be used to search for repetitions directly from these sources. Although continued monitoring with ASKAP or single-dish telescopes may reveal additional bursts from FRBs, these will not provide unambiguous host identifications. Detections of additional bursts with targeted phased-array observations with the VLA would not only demonstrate repetitions, confirming the existence of a class of repeating FRBs, but would also immediately lead to a host identification. This technique may therefore provide a novel framework for identifying counterparts and localizing future FRBs. However, in the absence of repetitions or very precise localizations, definitive associations remain challenging, particularly due to the broad region of parameter space occupied by AGN.

We thank the referee for helpful comments. The Berger Time-Domain Group at Harvard is supported in part by the NSF through grant AST-1714498, and by NASA through grants NNX15AE50G and NNX16AC22G. This research has made use of the FRB Catalog (http://www.astronomy.swin.edu.au/pulsar/frbcat/) and NASA's Astrophysics Data System.

Software: CASA (McMullin et al. 2007), pwkit (Williams et al. 2017).

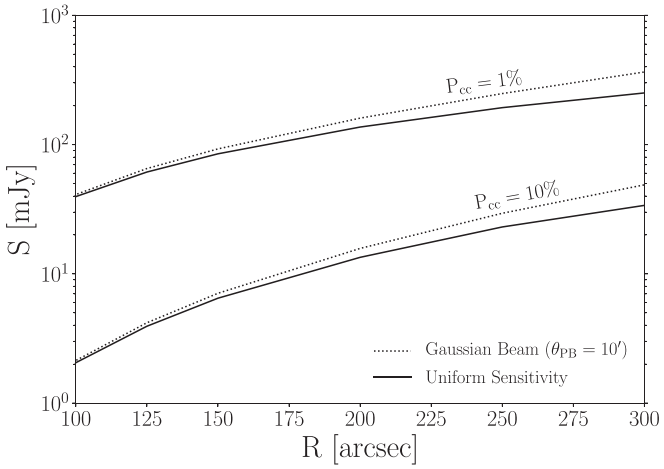

Figure 5. Comparison of 1% and 10% probability contours assuming a uniform-sensitivity beam and a Gaussian primary beam with $\theta_{PB} = 10'$.

Appendix
Accounting for the Primary Beam Response

In Section 2, the chance coincidence probability is calculated assuming uniform sensitivity over a region with a 1σ localization radius given by R_{FRB}. However, in typical radio observations, sensitivity is not spatially uniform. Consequently, the number density of detectable point sources decreases. In the common case of a Gaussian primary beam, the limiting flux density is given by $S_{lim} = S \cdot e^{-r^2/2\sigma_{PB}^2}$, where r is the distance from the pointing center, $\sigma_{PB} \approx \theta_{PB}/2.4$, and θ_{PB} refers to the full-width at half power of the primary beam. For a given localization radius R and flux density S, the resulting chance coincidence probability P_{cc} therefore increases. In this scenario, the chance coincidence probability is given by:

$$P_{cc} = 1 - e^{-\int_0^R 2\pi r\, n(S \cdot e^{-r^2/2\sigma_{PB}^2})\, dr}. \quad (2)$$

We illustrate the effects of accounting for the primary beam response in Figure 5. Namely, we recalculate the chance coincidence probability using Equation (2), where we use, as an example, $\theta_{PB} = 10$ arcmin (representative of the VLA at 4.5 GHz). We find that in this regime, an accurate characterization of the beam produces results that are comparable to the uniform sensitivity case across the extent of the primary beam ($R = 300''$). For example, at $R = 300''$, using Equation (1), we find that a 1% chance coincidence probability occurs for a source flux density of $\approx$250 mJy. Conversely, in the case of a Gaussian beam, the same flux density corresponds to a $\approx$1.2% chance coincidence probability, where $P_{cc} = 1\%$ requires $S \approx 300$ mJy. We therefore conclude that our simplified beam-model analysis in Section 2 is sufficient in terms of characterizing P_{cc} and identifying the required localization precision for confident associations.

ORCID iDs

T. Eftekhari https://orcid.org/0000-0003-0307-9984
E. Berger https://orcid.org/0000-0002-9392-9681
P. K. G. Williams https://orcid.org/0000-0003-3734-3587

References

Afonso, J., Georgakakis, A., Almeida, C., et al. 2005, ApJ, 624, 135
Baldwin, J. A., Phillips, M. M., & Terlevich, R. 1981, PASP, 93, 5

Bannister, K. W., Shannon, R. M., Macquart, J.-P., et al. 2017, ApJL, 841, L12
Barger, A. J., Cowie, L. L., & Wang, W.-H. 2007, ApJ, 654, 764
Beloborodov, A. M. 2017, ApJL, 843, L26
Caleb, M., Flynn, C., Bailes, M., et al. 2017, MNRAS, 468, 3746
Champion, D. J., Petroff, E., Kramer, M., et al. 2016, MNRAS Letters, 460, L30
Chatterjee, S., Law, C. J., Wharton, R. S., et al. 2017, Natur, 541, 58
Condon, J. J. 1984a, ApJ, 287, 461
Condon, J. J. 1984b, ApJ, 284, 44
Condon, J. J., Cotton, W. D., Fomalont, E. B., et al. 2012, ApJ, 758, 23
Cordes, J. M., & Wasserman, I. 2016, MNRAS, 457, 232
Cornwell, T. J., Golap, K., & Bhatnagar, S. 2008, ISTSP, 2, 647
Deller, A. T., & Middelberg, E. 2013, AJ, 147, 14
Deng, W., & Zhang, B. 2014, ApJL, 783, L35
Eftekhari, T., & Berger, E. 2017, ApJ, 849, 162
Falcke, H., & Rezzolla, L. 2014, A&A, 562, A137
Fomalont, E. B., Kellermann, K. I., Cowie, L. L., et al. 2006, ApJS, 167, 103
Ioka, K. 2003, ApJL, 598, L79
Johnston, S., Taylor, R., Bailes, M., et al. 2008, ExA, 22, 151
Keane, E. F., Johnston, S., Bhandari, S., et al. 2016, Natur, 530, 453
Keane, E. F., Stappers, B. W., Kramer, M., & Lyne, A. G. 2012, MNRAS Letters, 425, L71
Kumar, P., Lu, W., & Bhattacharya, M. 2017, MNRAS, 468, 2726
Lawrence, E., Wiel, S. V., Law, C., Spolaor, S. B., & Bower, G. C. 2017, AJ, 154, 117
Lorimer, D. R., Bailes, M., McLaughlin, M. A., Narkevic, D. J., & Crawford, F. 2007, Sci, 318, 777
Lyubarsky, Y. 2014, MNRAS Letters, 442, L9
Lyutikov, M., Burzawa, L., & Popov, S. B. 2016, MNRAS, 462, 941
Machalski, J., & Condon, J. J. 1999, ApJS, 123, 41
Marcote, B., Paragi, Z., Hessels, J. W. T., et al. 2017, ApJL, 834, L8
McMullin, J. P., Waters, B., Schiebel, D., Young, W., & Golap, K. 2007, in ASP Conf. Ser. 376, Astronomical Data Analysis Software and Systems XVI, ed. R. A. Shaw, F. Hill, & D. J. Bell (San Francisco, CA: ASP), 127
McQuinn, M. 2014, ApJL, 780, L33
Metzger, B. D., Berger, E., & Margalit, B. 2017, ApJ, 841, 14
Michilli, D., Seymour, A., Hessels, J. W. T., et al. 2018, Natur, 553, 182
Murase, K., Kashiyama, K., & Mészáros, P. 2016, MNRAS, 461, 1498
Nicholl, M., Berger, E., Margutti, R., et al. 2017a, ApJL, 845, L8
Nicholl, M., Berger, E., Margutti, R., et al. 2017b, ApJL, 835, L8
Nicholl, M., Williams, P. K. G., Berger, E., et al. 2017c, ApJ, 843, 84
Ofek, E. O. 2017, ApJ, 846, 44
Padovani, P., Bonzini, M., Kellermann, K. I., et al. 2015, MNRAS, 452, 1263
Padovani, P., Giommi, P., Landt, H., & Perlman, E. S. 2007, ApJ, 662, 182
Padovani, P., Mainieri, V., Tozzi, P., et al. 2009, ApJ, 694, 235
Pardo, K., Goulding, A. D., Greene, J. E., et al. 2016, ApJ, 831, 203
Park, S., Yang, J., Oonk, J. B. R., & Paragi, Z. 2016, MNRAS, 465, 3943
Petroff, E., Barr, E. D., Jameson, A., et al. 2016, PASA, 33, 45
Piro, A. L. 2016, ApJL, 824, L32
Popov, S. B., & Postnov, K. A. 2013, arXiv:1307.4924
Reines, A. E., Greene, J. E., & Geha, M. 2013, ApJ, 775, 116
Reines, A. E., Sivakoff, G. R., Johnson, K. E., & Brogan, C. L. 2011, Natur, 470, 66
Sault, R. J., & Wieringa, M. H. 1994, A&AS, 108, 585
Schinckel, A. E., Bunton, J. D., Cornwell, T. J., Feain, I., & Hay, S. G. 2012, Proc. SPIE, 8444, 84442A
Schlafly, E. F., & Finkbeiner, D. P. 2011, ApJ, 737, 103
Seymour, N., Dwelly, T., Moss, D., et al. 2008, MNRAS, 386, 1695
Shannon, R. M., & Ravi, V. 2017, ApJL, 837, L22
Smolčić, V., Schinnerer, E., Scodeggio, M., et al. 2008, ApJS, 177, 14
Spitler, L. G., Cordes, J. M., Hessels, J. W. T., et al. 2014, ApJ, 790, 101
Spitler, L. G., Scholz, P., Hessels, J. W. T., et al. 2016, Natur, 531, 202
Tendulkar, S. P., Bassa, C. G., Cordes, J. M., et al. 2017, ApJL, 834, L7
Thornton, D., Stappers, B., Bailes, M., et al. 2013, Sci, 341, 53
van Leeuwen, J. 2014, in The Third Hot-wiring the Transient Universe Workshop (HTU-III), ed. P. R. Wozniak et al. (Menlo Park, CA: SLAC), 79
Varenius, E., Conway, J. E., Martí-Vidal, I., et al. 2014, A&A, 566, A15
Vega, O., Clemens, M. S., Bressan, A., et al. 2008, A&A, 484, 631
Wang, J.-S., Yang, Y.-P., Wu, X.-F., Dai, Z.-G., & Wang, F.-Y. 2016, ApJL, 822, L7
Williams, P. K. G., & Berger, E. 2016, ApJL, 821, L22
Williams, P. K. G., Clavel, M., Newton, E., & Ryzhkov, D. 2017, pwkit: Astronomical utilities in Python, Astrophysics Source Code Library, ascl:1704.001
Zhang, B. 2016, ApJL, 827, L31